NiO–CGO in situ nanocomposite attainment: One step synthesis

Beatriz Cela [a,*], Daniel A. de Macedo [a], Graziele L. de Souza [b], Antonio E. Martinelli [a], Rubens M. do Nascimento [a], Carlos A. Paskocimas [a]

[a] Materials Science and Engineering Postgraduate Program – PPGCEM, Federal University of Rio Grande do Norte, Natal 59072-970, Brazil
[b] Ceramic Laboratory – DEM, Federal University of Rio Grande do Norte, Natal 59072-970, Brazil

ABSTRACT

The CeO_2-based electrolyte low temperature SOFCs require special electrodes with a higher performance and compatibility. The performance of the CeO_2-based composite anodes depends on microstructural features such as particle size, tripe phase boundaries (TPB), surface area, and percolation. Some of the primary parameter can be manipulated during the materials synthesis. In this work the compound $NiO–Ce_{0.9}Gd_{0.1}O_{1.95}$ (NiO–CGO), used as anode in SOFC, was synthesized by two different processes. Both of them are based on the polymeric precursor method. Characterized by simultaneous thermogravimetry-differential thermal analysis, X-ray diffraction, scanning electron microscopy, Fourier transform infrared spectroscopy and dilatometry. The refinement of the XRD data indicated that the composite sample synthesized by the process called "one step synthesis" produced smaller crystallite size in comparison to the sample attained by the two steps process. Simple preliminary performance tests were done with single cells in which such I–V curves indicated that the cell with one step anode had better performance. "One step synthesis" product, in situ nanocomposite, presented similar fine grained particle sizes for both phases Ni and CGO, which would be beneficial to the electrochemical activity, also indicated by first performance tests.

© 2010 Elsevier B.V. Open access under the Elsevier OA license.

1. Introduction

Solid oxide fuel cells (SOFCs) are unique because of the ability to use a wide range of fuels, including natural gas, biogas, diesel, methanol, DME and ethanol. The type of fuel with which a SOFC is able to operate is largely dependent upon the anode [1–3]. Gases rich in hydrogen and containing carbon monoxide do not need to have additional steps to clean the gas [4,5]. Direct utilization of hydrocarbons such as natural gas, propane and other liquid fuels without pre-reforming can significantly reduce the system cost and is therefore highly desirable. The conventional Ni-based anode is prone to promoting carbon formation in handling steam-free hydrocarbons besides the catalyst oxidation reaction of the fuel [2].

Different from other types of fuel cells, a SOFC stack can be projected to operate in a temperature range from 500 °C to 1000 °C. The operational temperature is mainly influenced by the available solid electrolytes properties. The solid electrolytes' specific ionic conductivity changes with the temperature [5]. The low- and intermediate-temperature solid oxide fuel cell has been interesting for offering several advantages over the High Temperature SOFC (HT-SOFC). The relatively high operating temperature (800–1000 °C) of current designs would require more time and energy for start-up. By reducing the operating temperature these problems, as well as thermal compatibility among the components operational and production cost reduction and other helpful characterics become manageable [6].

According to Doshi et al. to reduce the operating temperature of SOFCs from 800 to 500 °C, there are two crucial points: reduction of the high ohmic resistance without decreasing electrolyte thickness below 5 μm and development of high-performance cathodes compatible with the electrolyte material. Operation at such a low-temperature should make decrease the level of requirements on both the seals and interconnects for an SOFC stack [6].

In the last decades, ceria has been doped with a variety of cations. The ceria structure is more compatible with trivalent cations and to exhibit a stable structure the ratio of cations radii and anions radii needs to be close to 0.70 [7]. The use of the rare-earth dopants (Y^{3+}, Gd^{3+}, Sm^{3+}, etc.) in ceria had being proved to have better CO_2 and H_2O stability than ceria doped with alkaline-earth oxides. In addition, the conductivities of ceria with trivalent dopants are much higher than those with bivalent dopants. Among those doped with rare-earth oxides and gadolinia- and samaria-doped ceria are widely considered to be the electrolytes for low and intermediate SOFCs because of their high conductivity and

* Corresponding author. Present address: Forschungszentrum Jülich GmbH, Central Technology Division (ZAT), Leo Brand Straße, D-52425 Jülich, Germany. Tel.: +49 176 61700342; fax: +49 241 538078769.
  E-mail address: b.cela@fz-juelich.de (B. Cela).

low activation energy [8,9]. Since the radius of Gd^{3+} is the closest one, gadolinium-doped ceria (CGO) solid solutions have been recognized to be leading electrolytes for use in intermediate- and low-temperature SOFC [8,9]. CeO_2-based SOFC are largely limited to low-temperature (below 600 °C) applications in which it is possible to suppress the electronic conduction in CeO_2 electrolytes and the propensity for dimensional change to an acceptable level. The electronic conduction and propensity for dimensional change are due to the presence of a variable Ce valence ($Ce^{3+} \rightarrow Ce^{4+}$), provoking oxygen loss and elevates the excess electronic conduction in reducing atmospheres [3].

Therefore doped ceria satisfies the first requirement proposed by Doshi et al. [6] to reduce the operating temperature of SOFC to 500 °C. Many research groups, as Doshi et al. [6], Hibino et al. [10], Eguchi et al. [11], Shao and Haile [12] demonstrated that for low-temperature operation of SOFC, a series of ceria-based oxides are very attractive due to their high ionic conductivities and that doped ceria can be a feasible electrolyte for low-temperature operation SOFC with fuels such as liquid methanol or hydrogen-containing gases.

Besides the requirements of electrochemical and electrocatalyst properties of the SOFC materials, the thermomechanical properties, for example, the coefficient of thermal expansion (CTE), morphological and geometric stability in different atmospheres, mechanical resistance are very important points in the material selection for application in relatively high temperatures. As well known in the planar SOFC the different functional materials, anode, electrolyte, cathode and interconnectors need to be joined. Which generates the main challenge for the SOFC research – find materials with similar coefficient of thermal expansion to avoid thermomechanical stresses due to the thermal cycling. Traditionally the materials used that had compatible CTE are the electrolyte YSZ ($10 \times 10^{-6}\,K^{-1}$), cermet anode Ni/YSZ ($12 \times 10^{-6}\,K^{-1}$), cathode LSM – $(La,Sr)MnO_3$ or LSCF – $(La,Sr)(Co,Fe)O_3$ ($12 \times 10^{-6}\,K^{-1}$) and interconnector plates CroFer22APU [13]. For this reason, the development and use of new electrolytes based in ceria generates the need of development of special electrodes with a higher performance and chemical and thermomechanical compatibility.

The introduction of Ni in a doped ceria matrix can be a good way to achieve enough electronic conductivity to avoid electric losses. Furthermore it acts as a catalytic material to the methane crack reaction [14–16]. Another noticeable advantage for CeO_2-based anodes is the exceptional tolerance to higher sulfur levels in the fuel stream. This is probably the result of a stronger chemical affinity between CeO_2 and S than between Ni and S. Under typical SOFC operating conditions, Ce_2O_2S is thermodynamically stable and constantly keeps S away from Ni, leaving Ni uncovered by S [2].

Demanded functions of the gadolinium doped cerium oxide particles $Ce_{x-1}Gd_xO_{2-x/2}$ (CGO) in this ceramic–metal composite (cermet) Ni–CGO are: supplying the Triple Phase Boundary (TPB) with oxide ions, avoid the Ni particles sinterization and control the thermal expansion coefficient between the anode cermet and the CGO electrolyte layer [15,17,18]. For its properties the cermet can be used as a high performance electrode.

It is also widely accepted that the performance of cermet anodes is strongly depending on microstructural features such as phase composition, particle size, triple phase boundaries, surface areas, tortuosity and connectivity [19]. Therefore in this work a different synthesis methodology was developed to obtain $NiO–Ce_{0.9}Gd_{0.1}O_{1.95}$ nanocomposite with better microstructural features, as contact area between electrocatalyst (Ni) and ionic conductor (CGO), named as "one step synthesis". It was the synthesis of the NiO and CGO phases by one unique polymeric precursor's synthesis, in situ composite production. This methodology was compared to a second methodology previously studied – "two steps synthesis" – which consists of mixing of the NiO and CGO phases,

which were pre-synthesized by the polymeric precursor method. The synthesis methods were compared in terms of microstructural features such as phase composition, particle size and the characteristics of the materials produced have been investigated.

2. Experimental procedure

In this study the NiO–CGO ($NiO–Ce_{0.9}Gd_{0.1}O_{1.95}$) composite was prepared by the two different routes called "one step synthesis" and "two steps synthesis". To produce the composite by one step synthesis, the precursor resins of the CGO and NiO phases were previously obtained by the polymeric precursor method and then mixed to become one homogeneous resin. The resultant resin was expanded at 350 °C at a heating rate of $1\,°C\,min^{-1}$ and dwell time of 1 h. In contrast in the two steps synthesis procedure the composite was obtained by two separated polymeric precursor synthesis method, the CGO and the NiO precursor resins were expanded at 300 °C and 350 °C, respectively, at a heating rate of $1\,°C\,min^{-1}$ and dwell time of 1 h.
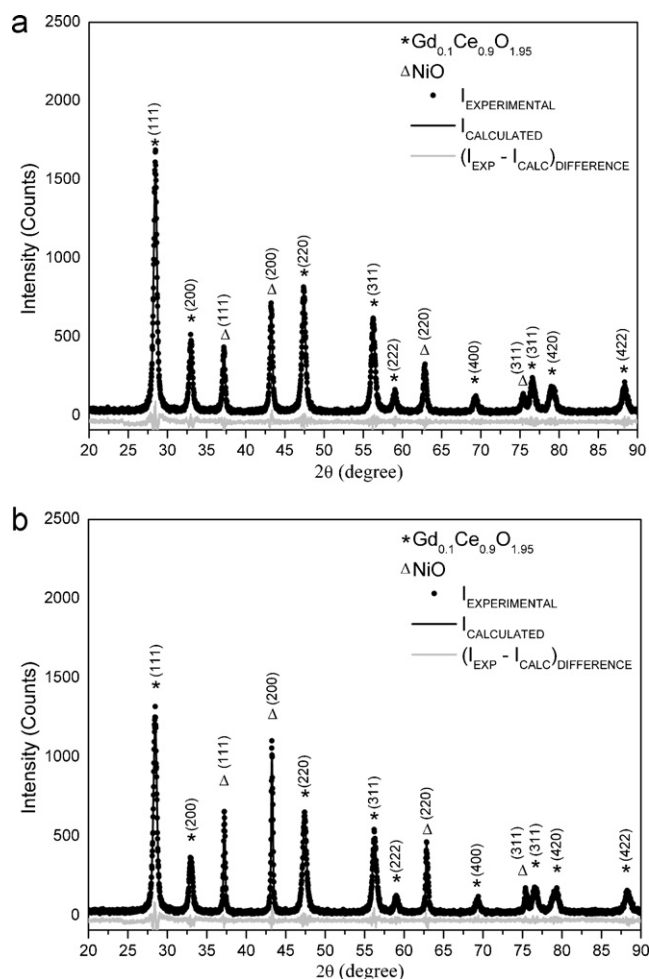
As a second step, CGO and NiO powders were mixed in a weight ratio of 1:1 and the mixture was ball-milled for 2 h under 60 rpm rotation. Expanded resins powders' preliminary analyses were made using a TG/DTA simultaneous analyzer (Model STA 409C, Netzsch), from 25 °C to 1000 °C and synthetic air atmosphere. Followed by calcination process previous determined by experiments 800 °C for 2 h, equal for all the powders.

All the experiments in this work had the polymeric precursor synthesis performed with the same proportion of citric acid:metallic cations, 3.5:1; and also the same rate of citric acid:ethylene glycol mass, respectively, 60:40. The starting materials used were cerium nitrate hexahydrate (VETEC, Brazil) 99.0%, gadolinium nitrate hexahydrate (Sigma–Aldrich) 99.9% and nickel nitrate hexahydrate (VETEC, Brazil) 98.0%. To reach approximately 39% of metallic phase in the final anode it was determined that 50% of NiO phase is necessary in the composite [18].

Samples of the two composite powders were prepared by compaction on a matrix with 8 mm in diameter, under 198 MPa uniaxial pressure. The pellets were sinterized in air at 1300 °C, heating rate used was $5\,°C\,min^{-1}$ for 0.5 h. Samples of the anode were also submitted to thermal treatment in H_2 pure atmosphere from room temperature to 900 °C, $5\,°C\,min^{-1}$ during 1 h, to reduce the NiO to metallic Ni and to be able to analysis this effect.

Characterization was done by X-ray diffraction (XRD), scanning electron microscopy (SEM) and Fourier transform infrared spectroscopy (FTIR). XRD analyses were performed by using X-ray diffractometer (XRD-6000, Shimadzu), using Cu Kα radiation, with 40 kV and 40 mA. By Rietveld XRD data refinement with the program BDWS-9807 [20] the present phases and crystallite average size (D_{XRD}) were calculated. Synthesized powders samples' morphologies were analyzed by SEM (SSX-550, Shimadzu), as well as the sintered composite microstructures. Sintered pellets were polished and thermally attacked to reveal the grain boundaries. The infrared spectra of the NiO–CGO composite made by both methods were recorded with FTIR (IR Prestige-21, Schimadzu) in the $400–4600\,cm^{-1}$ spectral range. A dilatometer (BP Engenharia RB-115, Brazil) was used to study the shrinkage behavior at a constant heating rate (CHR) of $3\,°C\,min^{-1}$ up to 1250 °C.

Furthermore, a first preliminary performance test was done to only qualitatively evaluate the prepared anodes in comparison to each other and a standard material, NiO–YSZ. Three single cells supported on commercial, 200 μm thick, YSZ electrolyte (Kerafol, Germany) with anode and cathode screen printing deposition were used for performance tests. To assemble the single cells, first the anode suspensions were printed and the half cells were sintered at 1250 °C for 4 h in the case of NiO–CGO one and two

Fig. 1. XRD patterns of NiO–Ce$_{0.9}$Gd$_{0.1}$O$_{1.95}$ composites synthesized by (a) one step synthesis and (b) two steps synthesis.

Table 1
Crystallographic parameters comparison of the both synthesis methods.

Parameters/phases	One step synthesis		Two step synthesis	
	Ce$_{0.9}$Gd$_{0.1}$O$_{1.95}$	NiO	Ce$_{0.9}$Gd$_{0.1}$O$_{1.95}$	NiO
$a = b = c$ (Å)	5.4155	4.1763	5.4180	4.1760
d (Å)	1.7619	1.6881	1.7624	1.6877
Volume (Å^3)	158.832	72.842	159.044	72.825
D_{XRD} (nm)	18.06	26.56	45.84	47.82
ε (%)	0.1997	0.1306	0.0695	0.0782
Weight (%)	50.40	49.60	48.56	51.44
Rwp (%)	14.19		16.25	
$Rexp$ (%)	11.25		12.47	
χ^2	1.26		1.30	

The diagrams (Fig. 1) show the crystalline state and the phases attained in both methods, one step synthesis (Fig. 1a) and two steps synthesis (Fig. 1b). No secondary phases are detected by X-ray diffraction after calcination of the composites at 800 °C for 2 h. A comparative study between the crystallographic parameters of the powders has been obtained by Rietveld refinement using the program BDWS-9807 (Table 1). Both composites exhibit the NiO and CGO phases with cubic fluorite type structures and space group Fm-3m (no. 225). The two steps synthesis powder shows higher crystallite sizes for both CGO and NiO phases, respectively, 60 and 65% higher than the composite attained by one step synthesis. The composition control has been investigated with respect to the weight content of each phase, showing that the one step synthesis method was better again. The microstrain (ε) values increased for CGO and NiO phases attained by one step synthesis compared to the two steps method. This can indicate that nickel element entered on the fluorite structure formed by gadolinium doped-ceria. Although to evaluate if there was entrance of nickel in the solid solution, it would be necessary to use other techniques. The values of χ^2 are between 1.26 and 1.30, attesting to the reliability of the Rietveld refinements.

The NiO–CGO composite FTIR spectra (Fig. 2) shows that the absorption bands in low wave number region are associated to the oxygen–metal linkage. The enlarged bands in ~3500 cm^{-1} are attributed to the stretching vibration of the hydrogen-bonded OH groups present. The bands referents to water in the material (3420 cm^{-1}) were present in both samples. The carbon bands were nearly eliminated after the thermal treatment at 800 °C

steps anodes, and 1300 °C for 4 h for the NiO–YSZ anode. Later on the LSCF-SDC cathode was printed in each half cell and sintered at 950 °C for 4 h.

The performance was evaluated using an in-house test station. Each single cell was tested using dry hydrogen as fuel and oxygen as oxidant, in the ratio of 40 ml min^{-1} H$_2$ and 40 ml min^{-1} O$_2$. The current–voltage characteristics of the cells were measured using linear sweep voltammetry (LSV) over a temperature of 850 °C. The microstructure and morphology of the single cell with one step anode after performance testing was examined by scanning electron microscopy (SEM).

3. Results and discussion

Characteristic differences of powders synthesized by different methods could be noticed along the characterization process. The composite can be attained by the polymeric precursor method, even from the resin mixture in the case of one step synthesis, as Ni does not form solid solution with the cerium or gadolinium oxides, although literature does not have a consensus about the Ni solubility in CeO$_2$ [14].

The possibility of attainment of crystalline CGO, NiO and NiO–CGO phases starting at 650 °C was observed by thermal analyses. Therefore, 800 °C was the chosen calcinations temperature for the compositions due to XRD data showing better crystallized phases at this temperature.
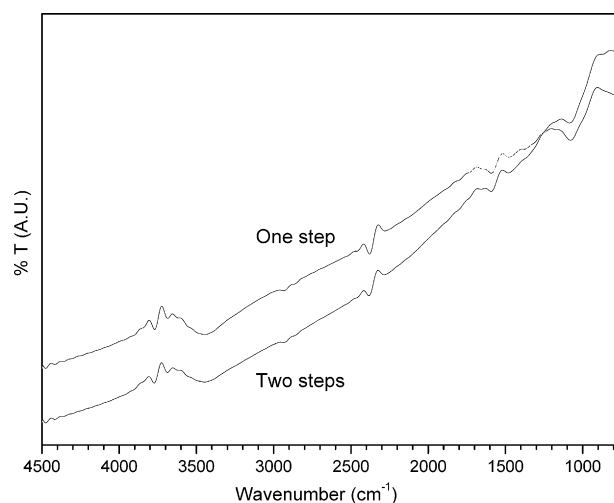

Fig. 2. Infrared spectroscopy of the CGO–NiO for samples produced by one step and two steps synthesis.

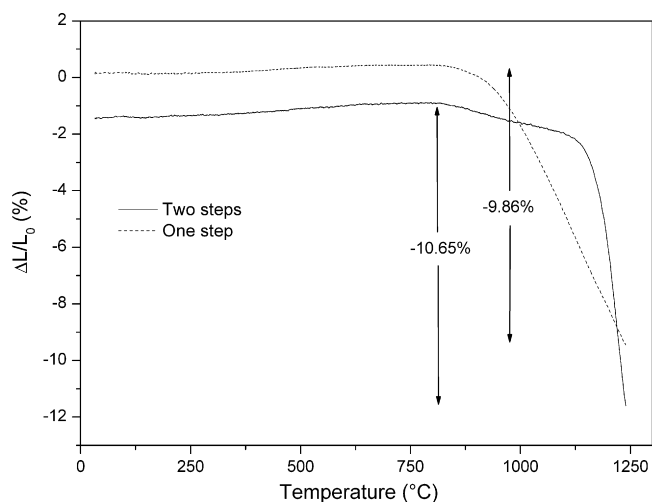**Fig. 3.** Dilatometry analyses of the composites sinterability.

Fig. 4. SEM micrographs of the NiO–CGO powders obtained by (a) two steps synthesis and (b) one step synthesis.

for 2 h. Indicating a residual carbon some bands still can be found in the calcinated samples, for example associated to carboxylate anion (COO^-) stretching and the C=O groups or to stretching vibration of the C–O bonds ($1620\,cm^{-1}$, $1389\,cm^{-1}$ and $1060\,cm^{-1}$).

Dilatometric analyses were performed to verify the sintering behavior of the composite samples (Fig. 3) as this is a very important step of the composite processing. The result for the material processed by two steps synthesis shows that the sintering process occurs around 1200 °C, lower than previously reported in literature for the same composition and ratio of NiO and CGO [14]. As for the overall shrinkage in the testing range from room temperature to 1250 °C, it is mere 9.86% for the one step sample, while the total shrinkage of two steps sample reaches 10.65%. As the slope at the end of the curve for two steps sample is steep, it is indicated that the shrinkage is far from ending at 1250 °C. The curve for one step sample inclines more gently as it does in the two steps sample, although the shrinkage is not finished yet. As certain porosity on the pressed sample was desired, the sintering conditions chosen were 1300 °C only for 30 min, also avoiding grain growth.

Both synthesis methods, one step synthesis (Fig. 4a) and two step synthesis (Fig. 4b), can efficiently to produce nanometric-sized powders with thermal treatment of 800 °C for 2 h (Fig. 4). The composites powders had different morphology according to each method though.

A higher efficiency of the one step synthesis method was verified by the BSE images of the sintered composites, one step synthesis (Fig. 5a) and two step synthesis (Fig. 5b). The one step synthesized composite was attained a microstructure consisting of homogeneously dispersed NiO and CGO phases. For the composite obtained by one step synthesis it can be also seen that both the dark and white domains are continuous, indicating a large presence of well-connected grains of NiO–NiO and CGO–CGO in relation to the obtained composite by another method. The relationship of the primary microstructure parameters with the more complex topological features (triple phase boundary length TPBL, and specific surface area SSA) is crucial to optimize and improve the anodic performance [19,21].

By the images (Fig. 5) the porosity and the particle size of the sintered samples can be estimated. The particles sizes were similar in both NiO and CGO phases, respectively, 160 and 150 nm for the one step method obtained powder, while for the two steps method the particles sizes were, respectively, 210 and 155 nm. According to the
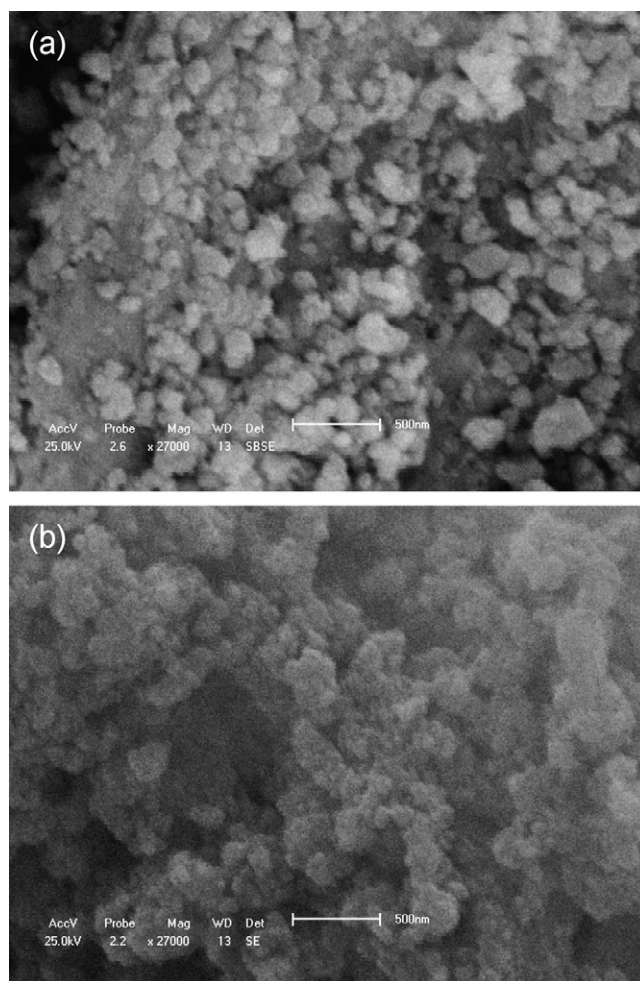
SEM images the apparent porosity is higher on the one step anode than in the two steps anode. This was confirmed by Archimedes' method for the one step and two steps anode before reduction, in which the results were, respectively, 22% and 3%. After reduction the anode is supposed to have a increase of porosity due to the reduction of volume of the NiO to Ni metal. The porosity of these anode still need to manipulated to better control it to the desirable ranges.

Through the LSV technique qualitative information about electrochemical activity was acquired. The cell voltages and power densities of the single cells prepared from the NiO–CGO one step anode, NiO–CGO two steps anode and NiO–YSZ standard anode (Fig. 6) revealed the maximum power densities were for the single cell composed by one step anode, This result is higher than that with a single cell prepared from two steps anode, as well as the one with NiO–YSZ anode. It is possible to compare qualitatively these first results and affirm that the one step anode is qualitatively better than the two steps version or the NiO–YSZ standard material. Although the voltage and power density values cannot be compared to the theoretical values because of the thick (200 μm) electrolyte used as cell support and also the experimental composite cathode used, LSCF-SDC.

Ni–CGO one step fracture surface was observed at the SEM after performance testing (Fig. 7). A uniform dispersion of the nickel phase and homogeneous porous microstructure were observed in the one step anode. The homogeneous microstructure is in

(a)

(b)
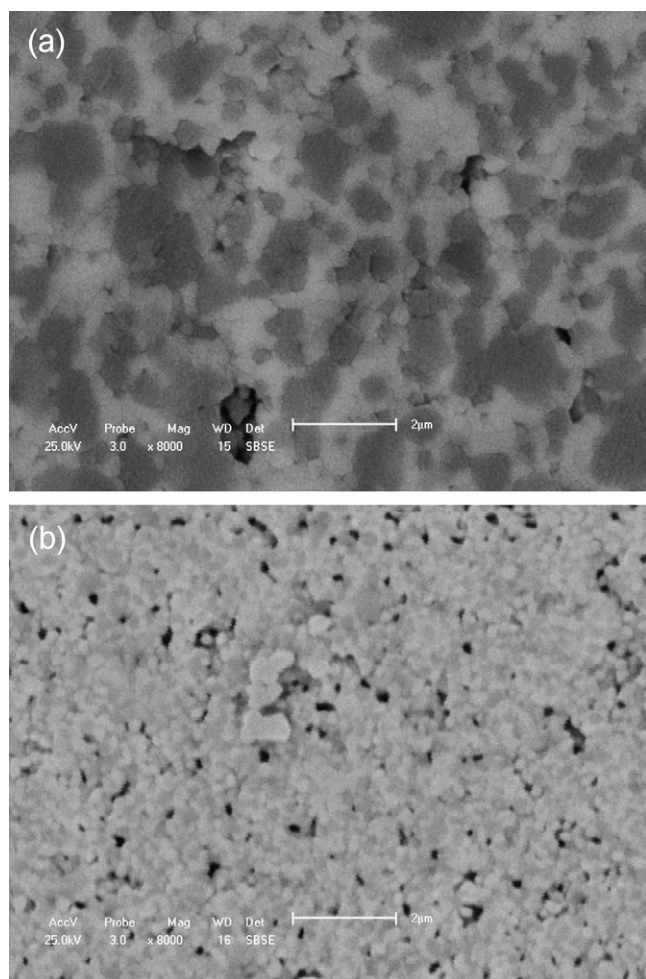
Fig. 5. BSE images of the NiO–CGO composites sintered at 1300 °C. Specimens obtained by (a) two steps synthesis and (b) one step synthesis.

agreement with the images showed above from the non-reduced composite anode. Once more the result indicates a large presence of well-connected grains of Ni–Ni, CGO–CGO and Ni–CGO, which are good for the TPB improvement.
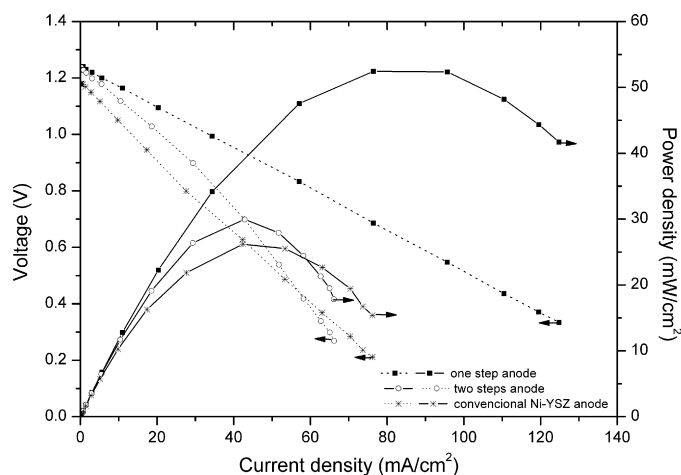
Fig. 6. *I–V* and *I–P* characteristics at 850 °C of the single cells LSCF-SDC//YSZ (cathode/electrolyte) varying the anode: Ni–CGO one step, Ni–CGO two steps and Ni–YSZ.
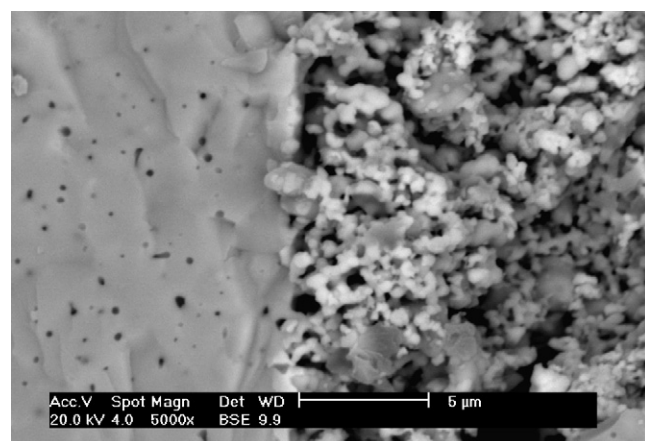
Fig. 7. SEM micrographs of the Ni–CGO one step anode after performance test.

4. Conclusion

The results showed that the two steps synthesis and the one step synthesis methods were successful to produce the NiO–CGO composite; and that the composite precursor's particles (pre calcinated) are essential to the achievement of a good nano or sub micrometric composite. Both methods are suitable for anode material production. Although by one step synthesis smaller initial particles size were obtained. Homogeneity and absence of agglomeration or phase segregation were also characteristics found in the powder synthesized and in the reduced anode made by one step synthesis. The similar densification behavior between the two phases can also be related to the initial particles size. In the sintered in situ composite the Ni percolating phase is good in the electronic conductivity, which was also indicated by the performance test. Together with the morphologic characteristics of the powders it is notable that the material processed in this way is a good candidate to SOFC anode. Comparing the in situ composite with the one synthesized by two steps, the in situ has many advantages: in example the homogeneous nanometric particles size of both phases increase the TPB because of particle–particle punctual contact, could mean a possible cell increase of efficiency. There is also Ni coalescence and sintering inhibition because of the good distribution in the ceramic matrix, nano and submicrometric particles size. Nevertheless, the interface between nickel and pore does not only representing the catalytically active surface, but it also represents the limiting factor for the formation of the TPB and therefore the "one step synthesis" anode still can be improved by controlling the pores formation an percolation.

Acknowledgment

References

[1] P. Piroonlerkgul, N. Laosiripojana, A.A. Adesina, S. Assabumrungrat, Chem. Eng. Process. 48 (2) (2009) 672.
[2] I. Kang, Y. Kang, S. Yoon, G. Bae, J. Bae, Int. J. Hydrogen Energy 33 (21) (2008) 6298.
[3] K. Huang, J.B. Goodenough, Solid Oxide Fuel Cell Technology: Principles, Performance and Operations, CRC Press, USA, 2009.
[4] S.C. Singhal, Solid Oxide Fuel Cells VI, PV 99-19, The Electrochemical Society, Inc., Pennington, NJ, USA, 1999, pp. 39–51.
[5] B.C.H. Steele, A. Heinzel, Nature 414 (2001) 345.
[6] R. Doshi, V.L. Richards, J.D. Carter, X. Wang, M. Krumpelt, J. Electrochem. Soc. 146 (4) (1999) 1273.
[7] C. Peng, Y. Zhang, Z.W. Cheng, X. Cheng, J. Meng, J. Mater. Sci. 13 (2002) 757.

[8] B.C.H. Steele, Solid State Ionics 129 (2000) 95.
[9] J.W. Fergus, J. Zhang, X. Li, D.P. Wilkinson, R. Hui, Solid Oxide Fuel Cells: Materials Properties and Performance, CRC Press, 2009.
[10] T. Hibino, A. Hashimoto, T. Inoue, J. Tokuno, S. Yoshida, M. Sano, Science 288 (2000) 2031.
[11] K. Eguchi, T. Setoguchi, T. Inoue, H. Arai, Solid State Ionics 52 (1–3) (1992) 165.
[12] Z. Shao, S.M. Haile, Nature 431 (2004) 170.
[13] F. Tietz, Ionics 5 (1999) 129, doi:10.1007/BF02375916.
[14] P. Datta, P. Majewski, F. Aldinger, J. Alloys Compd. 455 (2008) 454.
[15] V. Gil, J. Tartaj, C. Moure, Ceram. Int. 35 (2009) 839.

[16] S. Zha, W. Rauch, M. Liu, Solid State Ionics 166 (2004) 241.
[17] T. Ishihara, T. Shibayama, H. Nishiguchi, Y. Takita, Solid State Ionics 132 (2000) 209.
[18] V. Gil, C. Moure, J. Tartaj, J. Eur. Ceram. Soc. 27 (2007) 4205.
[19] L. Holzer, B. Münch, B. Iwanschitz, M. Cantoni, Th. Hocker, Th. Graule, J. Power Sources (2010), doi:10.1016/j.jpowsour.2010.08.006.
[20] R.A. Young, A.C. Larson, C.O. Paiva-Santos, User's Guide to Program DBWS-9807A for Rietveld Analysis of X-ray and Neutron Powder Diffraction Patterns with a PC and Various other Computers, School of Physics, Georgia Institute of Technology, Atlanta, GA, USA, 2000.
[21] C.W. Sun, U. Stimming, J. Power Sources 171 (2007) 247.